A LOW-COST, IN SITU RESISTIVITY AND TEMPERATURE MONITORING SYSTEM

Laura Sherrod[a], William Sauck[b], and D. Dale Werkema Jr.[c]

[a]Physical Sciences Department
Kutztown University
Kutztown, PA 19530
sherrod@kutztown.edu

[b]Department of Geosciences
Western Michigan University
Kalamazoo, MI 49008

[c]U.S. EPA, Office of Research and Development
National Exposure Research Laboratory
Las Vegas, NV 89119

Keywords –

In situ characterization using nonstress-based methods (e.g., geophysical methods, TDR, etc.)

Economics of characterization, monitoring, and remediation efforts

Abstract

We present a low-cost, reliable method for long-term in situ autonomous monitoring of subsurface resistivity and temperature in a shallow, moderately heterogeneous subsurface. Probes, to be

left in situ, were constructed at relatively low cost with an electrode spacing of 5cm. Once installed, these were wired to the CR-1000 Campbell Scientific Inc. datalogger at the surface to electrically image infiltration fronts in the shallow subsurface. This system was constructed and installed in June 2005 to collect apparent resistivity and temperature data from ninety-six subsurface electrodes set to a pole-pole resistivity array pattern and fourteen thermistors at regular intervals of 30cm through May of 2008. From these data, a temperature and resistivity relationship was determined within the vadose zone (to a depth of approximately 1m) and within the saturated zone (at depths between 1m and 2m). The high vertical resolution of the data with resistivity measurements on a scale of 5cm spacing coupled with surface precipitation measurements taken at 3-minute intervals for a period of roughly three years allowed unique observations of infiltration related to seasonal changes. Both the vertical resistivity instrument probes and the data logger system functioned well for the duration of the test period and demonstrated the capability of this low cost monitoring system.

1.0 Introduction

While long-term geophysical monitoring provides a useful tool for the interpretation of subsurface hydrological properties and processes, the cost is often prohibitive. Resistivity measurements have long been utilized in hydrology as a non-invasive measurement technique. Whether utilized for determining water table depth (Reed et al. 1983), or observing preferential flow paths (Narbutovskih et al. 1996; Stephens 1996; Hagrey and Michaelsen 1999; Yang and LaBrecque 2000) resistivity data are valuable for non-invasive investigations. Additionally, contaminant and remediation characterization and monitoring efforts have also been imaged with this versatile technique (Daily and Ramirez 1995; Aaltonen and Olofsson 2002). The biodegradation of petroleum hydrocarbons has been observed and monitored through long-term resistivity experiments (Atekwana et al., 2000; Sauck, 2000; Werkema, 2002; Werkema et al., 2004). Other long-term three dimensional studies have been developed to characterize subsurface water flow and aquifer characteristics (Pfiefer and Andersen 1995; Cassiani et al. 2006). Steps toward the conversion of resistivity measurements into hydrological values have shown good success (Binley et al. 2002a; Binley et al. 2002b; Vanderborght et al. 2005; Linde et al. 2006; Johnson et al. 2009). Tracer studies have been performed in conjunction with electrical resistivity tomography (ERT) to identify the center of mass and concentration within tracer plumes (Kemna et al. 2002; Singha and Gorelick 2005; Singha and Gorelick 2006a; Singha and Gorelick 2006b). More recently, such resistivity devices have been employed through large collaborative efforts to monitor salt-water intrusions near important freshwater well sources (Ogilvy et al. 2009). While there is movement within this field of study toward autonomous systems, most of these studies do not employ such a system dedicated to on-site data collection for extended periods of time mostly due to the expense. Budget restrictive projects which require vadose zone measurements of water content do not have access to autonomous systems and are therefore confined to the use of other methods, including time-consuming manual data collection techniques. This work presents a low-cost method to reliably obtain long-term subsurface resistivity and temperature measurements.

2.0 Materials and Methods

The monitoring system is composed of two parts; the down hole in situ geophysical probe, which includes the electrodes for making contact with the subsurface; and the electronic instrument used for acquiring and recording the data.

Geophysical Probes

Four geophysical probes were constructed and installed to monitor subsurface water content dynamics through apparent resistivity (ϱ_a) measurements. These probes consisted of 19 mm (0.75 inch

O.D.) Schedule 80 PVC pipe with stainless steel band electrodes wrapped around the outside of the pipe at 5 cm intervals along the length of the pipe and secured with stainless steel screws. LaBrecque and Daily (2008) present a comprehensive analysis of the performance of several electrode materials and indicate that stainless steel performs reasonably well. Alternatively, Grimm et al. (2005) chose to use titanium electrodes due to titanium's resistance to weathering and to polarization. However, titanium's cost could be prohibitive to its use in low-cost systems, and for this reason was not chosen. Hence, the relatively low-cost option of stainless steel was chosen for this long-term monitoring experiment. The probes were constructed in order to fit in a direct push Geoprobe® hole, requiring an outside diameter no greater than 3.8 cm (1.50 inches). Wires to connect the electrodes to the datalogger and multiplexers were threaded through the interior of each probe. Thermistors were installed along the side of each probe at intervals of approximately thirty centimeters, or every six electrode spacings. Resistivity is a temperature-dependent physical property. These thermistors can be used to measure the subsurface temperature. This data allows for a temperature correction to be made to the resistivity data, thus providing a more accurate depiction of subsurface water content. Resistivity measurements are also impacted by the geometry of the electrode array. An empirical geometric factor for these probes was determined following the procedure outlined by Gronki and Sauck (2000). Figure 1 shows an example of a finished ϱ_a and temperature probe.

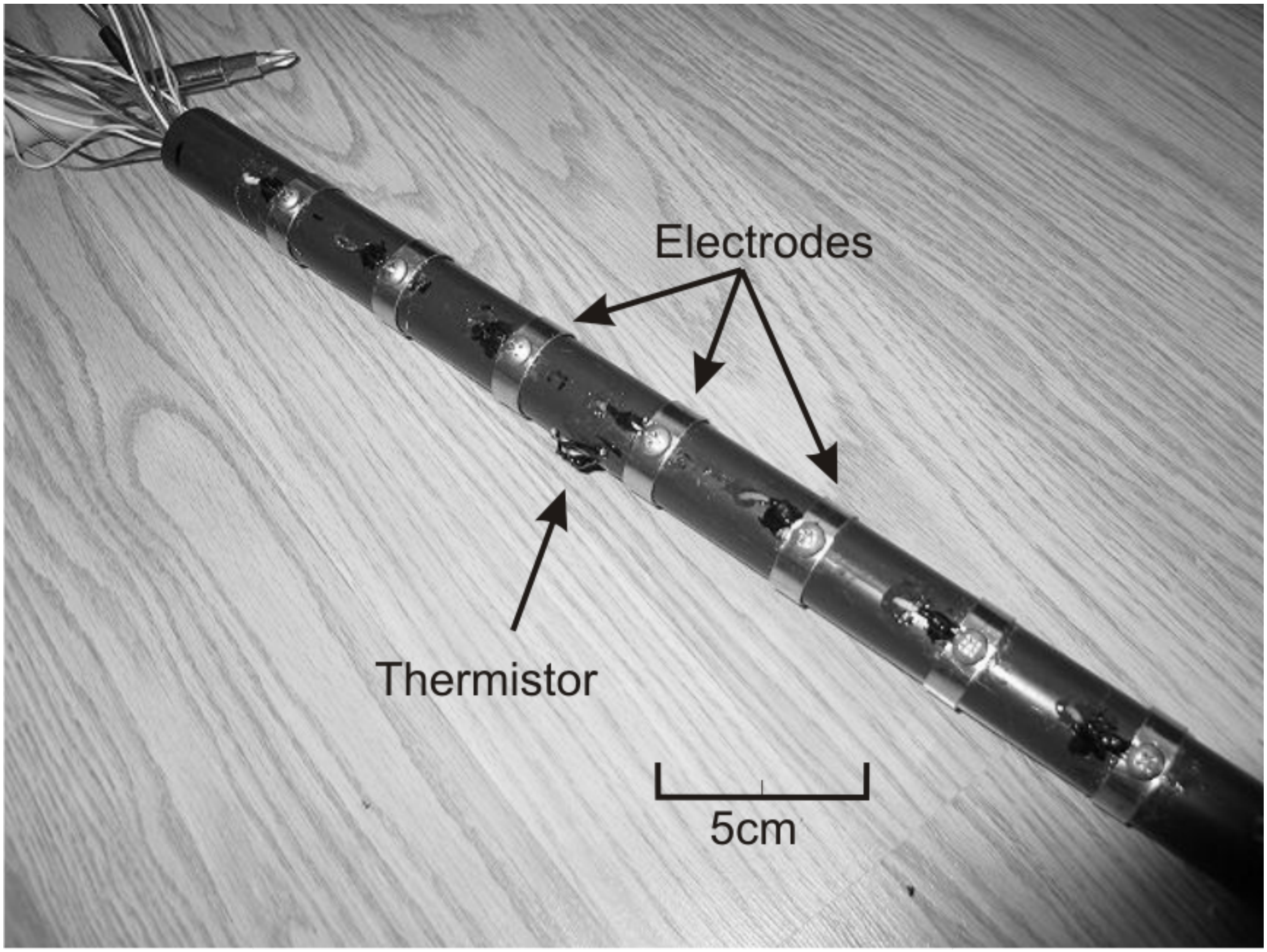

Figure 1: Resistivity and temperature probe with electrode spacing of 5cm and thermistors spaced at 30 cm.

Electronic Instrument System Design

To achieve our low-cost objective, the assemblage of the acquisition and datalogging system from off-the-shelf components was required. The cost of materials for this project was $7400 and probe construction required approximately forty hours. Commercially available resistivity meters do not contain cost effective components necessary for long-term (i.e., longer than one year) experiments.

Therefore, the CR1000 datalogger and all associated electronic components from Campbell Scientific, Inc. were chosen for low cost, versatility, and programming customization options. This datalogger has a pulse count channel that may be used to collect data from a rain gauge, can control numerous multiplexers, and has convenient programming and data retrieval options. Equally important is the capability of system alarms to trigger changes in the data collection mode (i.e. the frequency of recorded measurements), which is required to adapt for site dynamics

Although a telemetry option was available through Campbell Scientific, Inc., the data for this project were stored on a compact flash device within the datalogger to decrease overall system cost. Power was supplied by an MSX20 _20-Watt Solar panel which was used to recharge the PS100 12 V Power Supply. A tipping bucket rain gauge TE525WS was used to monitor daily and hourly rainfall totals. Four AM 16/32 relay multiplexers controlled the switching of electrodes and thermistors. The entire datalogging system was housed on-site in an ENC12/14 enclosure.

The CR1000 was programmed to control the four multiplexers to select the desired resistivity electrodes or thermistors. Using a precision 100 Ω resistor, a four wire half bridge measurement was performed to obtain the current for the resistivity measurements. A full bridge measurement was used to obtain the voltage for resistivity measurements, and a three wire half bridge, using a 1,000 Ω reference resistor, was utilized to obtain resistance values from the thermistors for the temperature data.

All data were stored in ASCII tables. Meta data included a time stamp and record number. The resistivity and temperature measurements were collected every four hours and recorded in a single table which contained the resistivity measurement position and the thermistor position. During precipitation events and throughout the subsequent four hours, the resistivity and temperature data were stored in a separate table, which includes rain gauge precipitation data recorded as the total precipitation for every three-minute scan cycle. Hourly and daily rain totals were also recorded by the system. Site visits, varying in frequency from once every few days to several months, were made to retrieve the data from the compact flash card and for system inspection.

Due to the depth to the water table and constraints with the datalogger capacity, the most practical design for experimental testing of this system was four individual probes; two of one-meter length and two of two-meter length. Probes 1 and 2 each contained sixteen electrodes. Probe 3 contained thirty-one electrodes and Probe 4 contained thirty-three electrodes. These lengths ensured that each probe crossed the transition between the vadose and saturated zones. The datalogger was connected to the probes and configured to record a series of Pole-Pole resistivity measurements from adjacent electrodes on the same probe which resulted in ninety-two measurement positions every four hours. Due to constraints of the data logging system and chosen multiplexers, not all possible combinations of electrode pairs on a given vertical array were used. Resistivity measurements were only taken from electrodes adjacent to each other on the same probe. During precipitation events and for the next four hours following such events, the frequency of the data collection cycle was increased to one cycle every three minutes. These data provided a very detailed image of infiltration events.

Field Site

The test site was in a hay field near a man-made pond constructed approximately fifty years ago in Pine Grove Township (Township 1 South, Range 13 West), Van Buren County, Michigan. The probes were installed vertically into the subsurface at an increasing distance from the pond and in a line perpendicular to the bank of the pond (Figure 2). Surface resistivity and ground penetrating radar (GPR) surveys along perpendicular lines verified the lateral continuity of soil layers prior to probe installation. When the pond was created, the excavated material was piled on top of the soil surface surrounding the new pond. A 5-cm (2-inch) diameter monitoring well was installed 0.5 m from each probe at the same distance from the pond to monitor water table levels at periodic intervals throughout the experiment. A time domain reflectometry (TDR) access tube was installed 0.5 m near each probe. Unfortunately, a necessary deviation from the recommended installation procedure for the access tube, due to the presence of large pebbles and cobbles, invalidated most of the TDR results and thus those are not presented. Additional attempts through the use of a neutron probe to obtain moisture content data also failed due to the inhomogeneities of the subsurface. As such, a qualitative measure of the subsurface moisture content was performed. Probes 1, 2, 3, and 4 were installed in a row perpendicular to the pond, at 3 m, 4 m, 6 m, and 9 m from the edge of the water at the time of installation. The water level of the pond was below 230 m (+/- 1 m) elevation throughout the duration of the experiment.

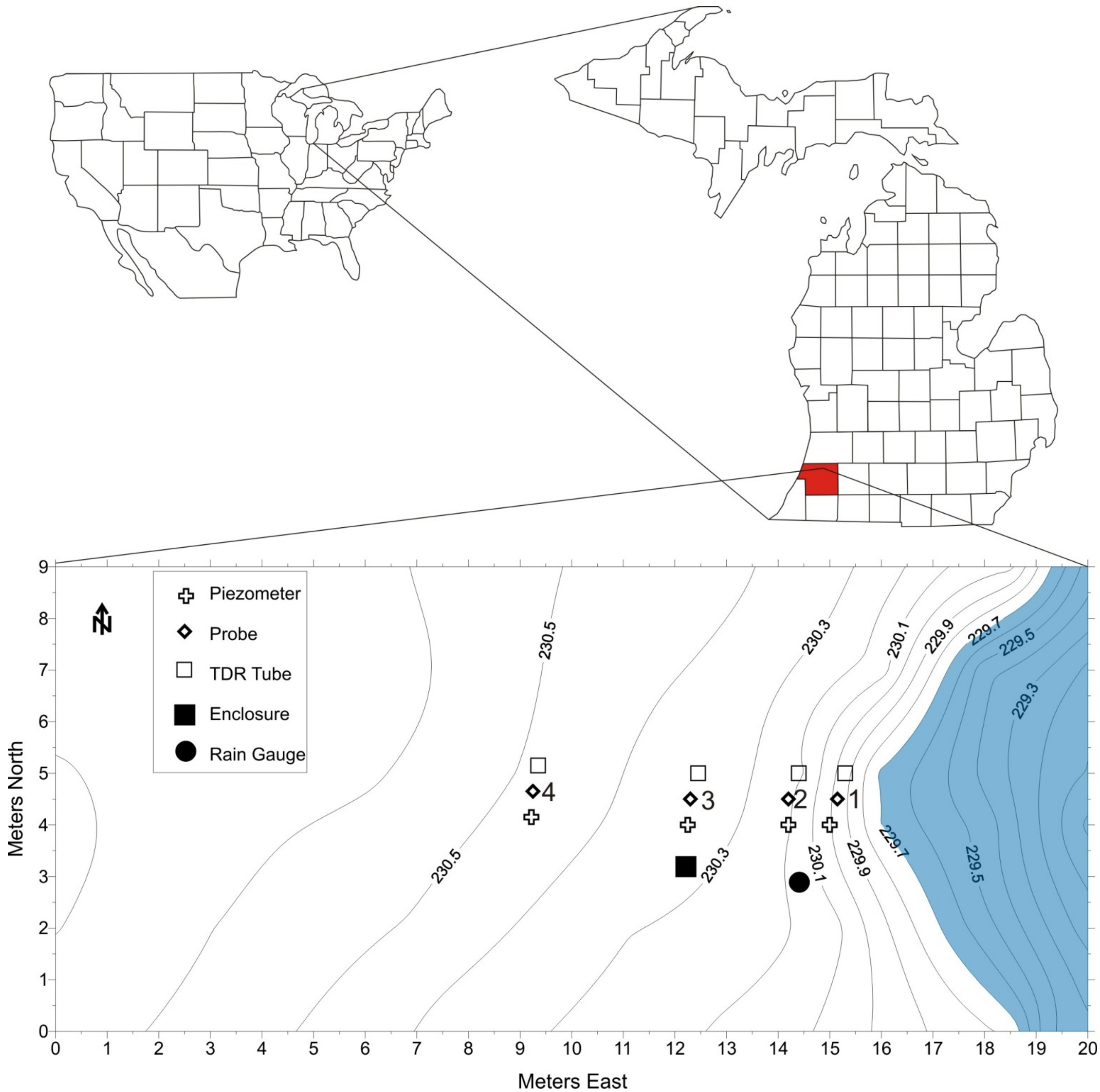

Figure 2: Site map showing location of probes. Surface water (shown in blue) was at 229.7m elevation at the time of installation.

Figure 3 shows the site representative subsurface soil distribution at the location of Probe 4 where the water table varied between approximately 230 m and 229 m. The Phi Value in this figure represents the log (base 2) of the grain size divided by the standard grain size of 1mm (Nichols, 1999) with high phi values corresponding to small sediment sizes and low phi values corresponding to large sediment sizes. High water table levels were recorded in the late winter and spring months while low water table levels were recorded in the late summer and fall months. The soil profile between Probes 2, 3, and 4 was laterally continuous. This uniform stratigraphy created an ideal situation for vertical resistivity measurements. The clay-rich layer from 229.4 m to 229.8 m elevation was likely the pre-excavation topsoil. This horizon was not present at the location of Probe 1, which was installed within the initial pond excavation area and was not submerged by surface water at any time during the testing period, due to low water levels. Sieve analysis of the cuttings from installation indicated a subsurface composed primarily of 0.25 mm to 0.5 mm sands with pebbles and cobbles found throughout the profile. The amount of fines, defined as anything smaller than 0.066 mm in diameter, remained below ten percent throughout the profile with the exception of the old pre-pond excavation topsoil layer which varied between ten and twenty percent.

The vadose zone hydrology was significantly influenced by the clay-rich horizon between 229.4 m and 229.8 m elevation. There were more fines within this old topsoil layer than found in the sandy layers above and below this horizon. This unit remained above the top of the water saturated zone for most of the duration of the testing. As such, it may be expected that during precipitation events, this horizon acted as a barrier to rapid infiltration below 229.4 m elevation.

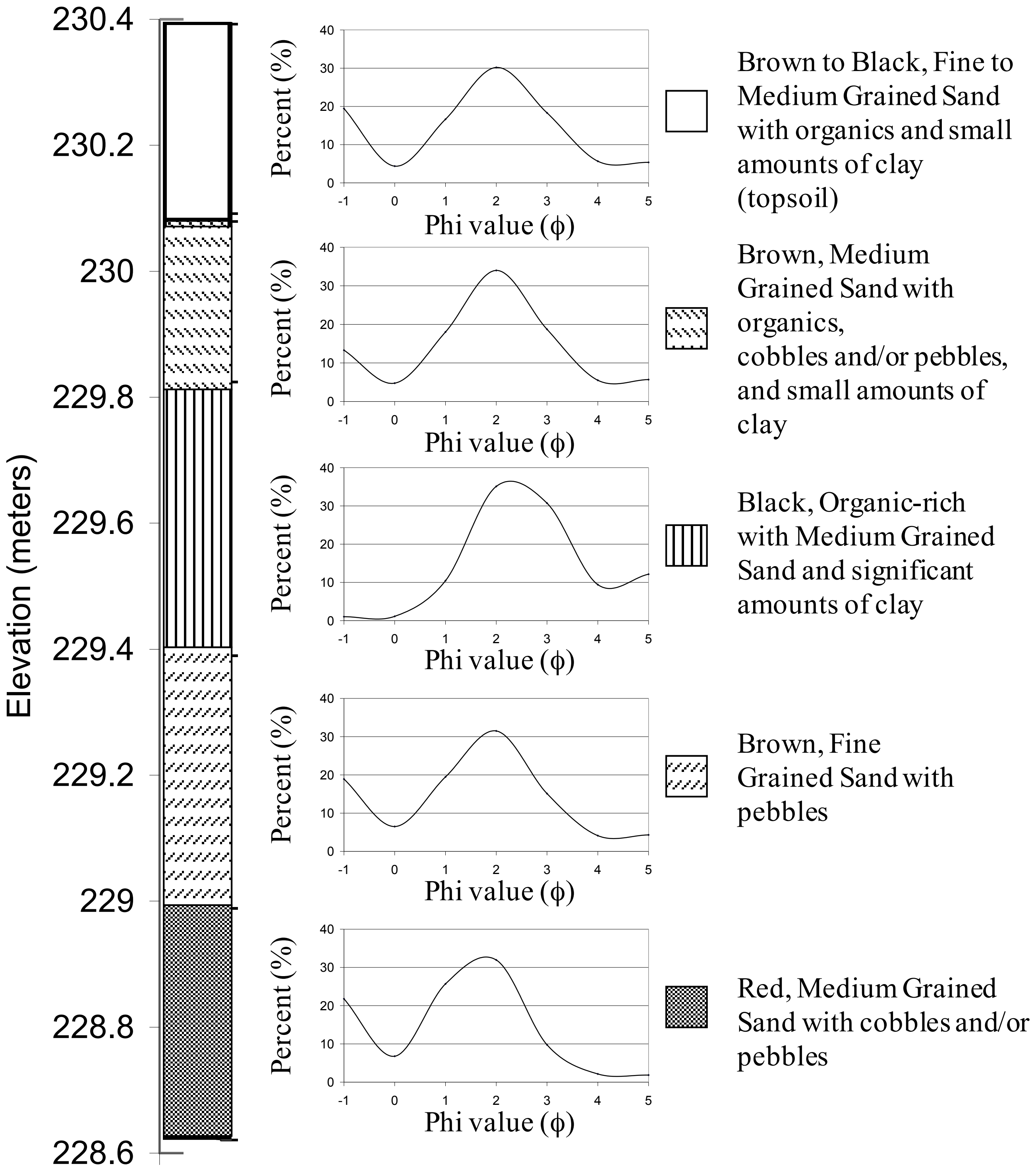

Figure 3: Lithologic description of the five distinct geologic units as observed at the location of Probe 4. These units are similar for the other probe locations.

3.0 Results/Discussion

Error Analysis

The experimental design was implemented and tested for nearly three years. Long-term results and inspection of the probes removed after the experiment indicate that this system was robust and endured over the course of the experiment. While a few of the electrodes exhibited some degradation caused by changes in the contact resistance over time, an effect which has been described in detail by LaBrecque and Sharpe (2006), there were no system failures and no substantial long-term drift identified in the data. Due to the low output voltage available through the CR1000, it was important to determine the accuracy of the resistivity measurements made with this system. Therefore, a comparison was made using a Syscal R2 resistivity meter. Measurements were made in the ranges of 79 Ωm to 160 Ωm with readings taken at all probes. All these resistivity measurements were within 10%, which was deemed acceptable. The measured values were similar despite the fact that the sphere of influence for each measurement taken by the CR1000 may be slightly diminished in comparison to a higher-output device.

Long-Term Results

Measurement modes were customized to identify transient events such as infiltration (one cycle of ninety-two resistivity measurements every three minutes) and for long-term monitoring using this same system. Figure 4 shows a typical data set representing one measurement from each resistivity measurement position every four hours at Probe 1 from November 2005 through January 2008. The apparent resistivity values have been converted to percent change of apparent resistivity from the 2006 average at each measurement location, which is every 5 cm based on the pole-pole 'a'-spacing configuration. To calculate this percent change for each measurement position, the average of all apparent resistivity data taken at each position during normal data collection (one measurement each four hours) was determined. This resulted in ninety-two individual 2006 averages, one average for each measurement position. Each average value was then used to determine the percent change for the other resistivity measurements at similar locations. In the absence of a calibration factor between resistivity and moisture content, this method allows a qualitative assessment of the subsurface saturation state as related to the measured resistivity. These data are presented without inversion and are therefore apparent resistivity, ρ_a, of the subsurface and not true resistivity. By plotting the apparent resistivity value between each electrode pair with depth, Figure 4 displays the percent change of the apparent resistivity of each measurement position with time. However, the appearance of the yearly cycle of high and low resistivity values corresponding to winter and summer months, respectively, clearly illustrates the impact of temperature upon the subsurface resistivity. The fact that these variations extend into the saturated zone demonstrates that these large, seasonal changes are not caused by water content variations, but by temperature changes. These long-term data illustrate seasonal trends, with high apparent resistivity in the winter months and low apparent resistivity in the summer months due to temperature variations.

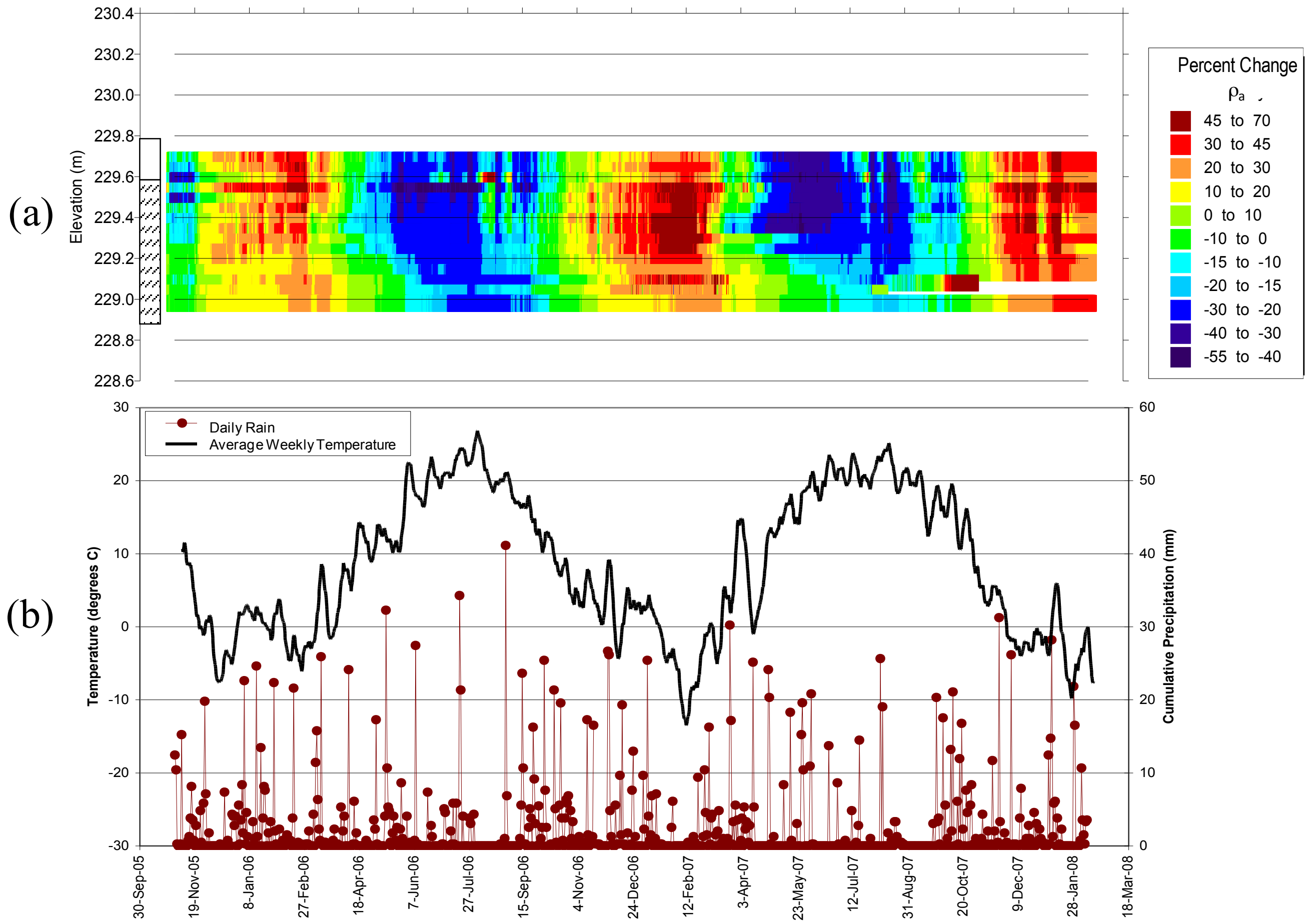

Figure 4: (a) Percent change of apparent resistivity for each measurement position from the 2006 average, (b) weekly average temperature, and daily rainfall totals at the location of Probe 1. The lithologic description is shown near the elevation axis and is similar to that shown in Figure 3.

Short-Term Results

These data also show short term infiltration patterns which are also influenced by the seasons. Imbibition and drainage cycles may be seen as high frequency variations imposed upon the low frequency temperature changes. Snow cover during the winter months at this site tends to decrease infiltration. Thus, the short-term decrease of apparent resistivity from precipitation events, which is caused by increased water content from infiltration, is minimized during these months. Figure 5 displays a detailed version of the infiltration events that occurred from November 2007 through January

2008 at Probe 1 and Probe 4. These data also reveal a faulty electrode connection apparent at 229.5m elevation at Probe 4. Nevertheless, the overall subsurface apparent resistivity changes are clearly evident. It is clear (Figure 5) that the stratigraphic unit with abundant fines at 229.4m to 228.8m elevation is a significant contributor to subsurface water flow. This is evident through the increased time that this unit maintains a lower apparent resistivity (i.e. the fines are holding on to the water that has infiltrated) compared to the upper unit which allows more rapid infiltration. An example of this may be seen in Figure 5 on 2 December 2007 when there was a precipitation event of over 26mm. The decreased apparent resistivity within the clay-rich unit persists for nearly four days following the precipitation event while the upper unit returns to higher apparent resistivity values by the next day after the precipitation.

It should be noted that the air temperature during the first half of the month of January 2008 was abnormally high, allowing for several infiltration events to occur in response to rainfall and snow melt. Overall, the impact of infiltration on the subsurface is subdued during the winter months, as seen in December 2007, due to the frozen ground surface and snow cover restricting infiltration. The data collection method of this system allows a visualization of surface temperature's influence upon the amount of infiltration. Figure 5 illustrates the impact and extent of precipitation events from 5-13 January and 28-29 January impacting the subsurface water content

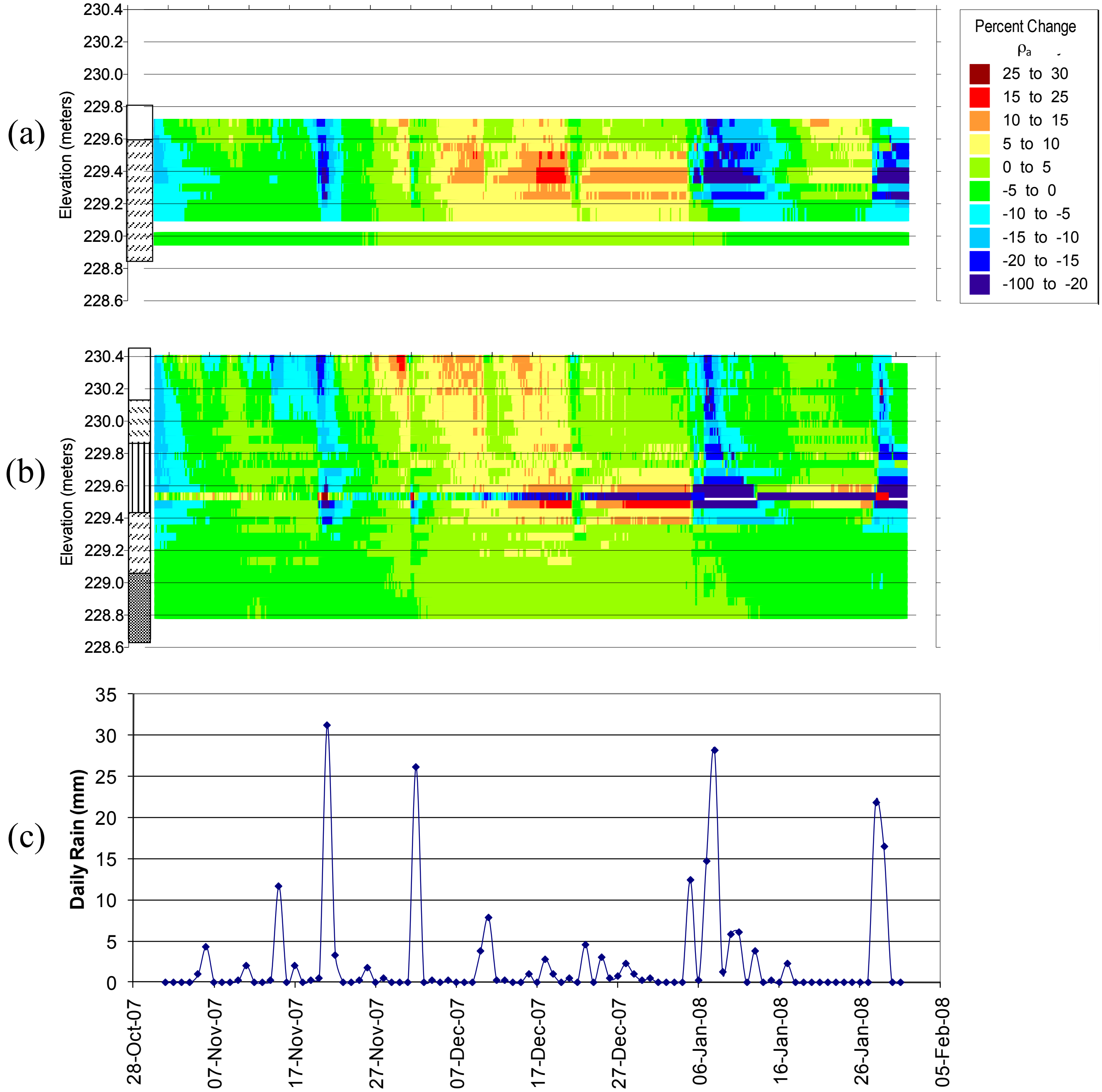

Figure 5: Infiltration front imaging at (a) Probe 1 and (b) Probe 4 showing the imbibition and drainage phases of the front with the (c) total daily rainfall below.

The robust design of this system allowed for greater resolution of infiltration fronts through the rapid data collection during and for four hours immediately following precipitation events. Figure 6 shows a series of natural infiltration events which occurred during the week, from 5 August 2007 through 13 August 2007. Initially, the upper portion of the subsurface was unsaturated, as shown by the high percent change of apparent resistivity indicated in red prior to the precipitation event of 5 August. The initial influx of water from this infiltration event was observed through an apparent resistivity value near the 2006 average by 6 August. Further precipitation and subsequent infiltration on 7 August may be seen as the apparent resistivity values decrease into the blue range of this color scale, indicating that they have achieved a greater level of saturation, and a subsequent decrease in apparent resistivity relative to the 2006 average.

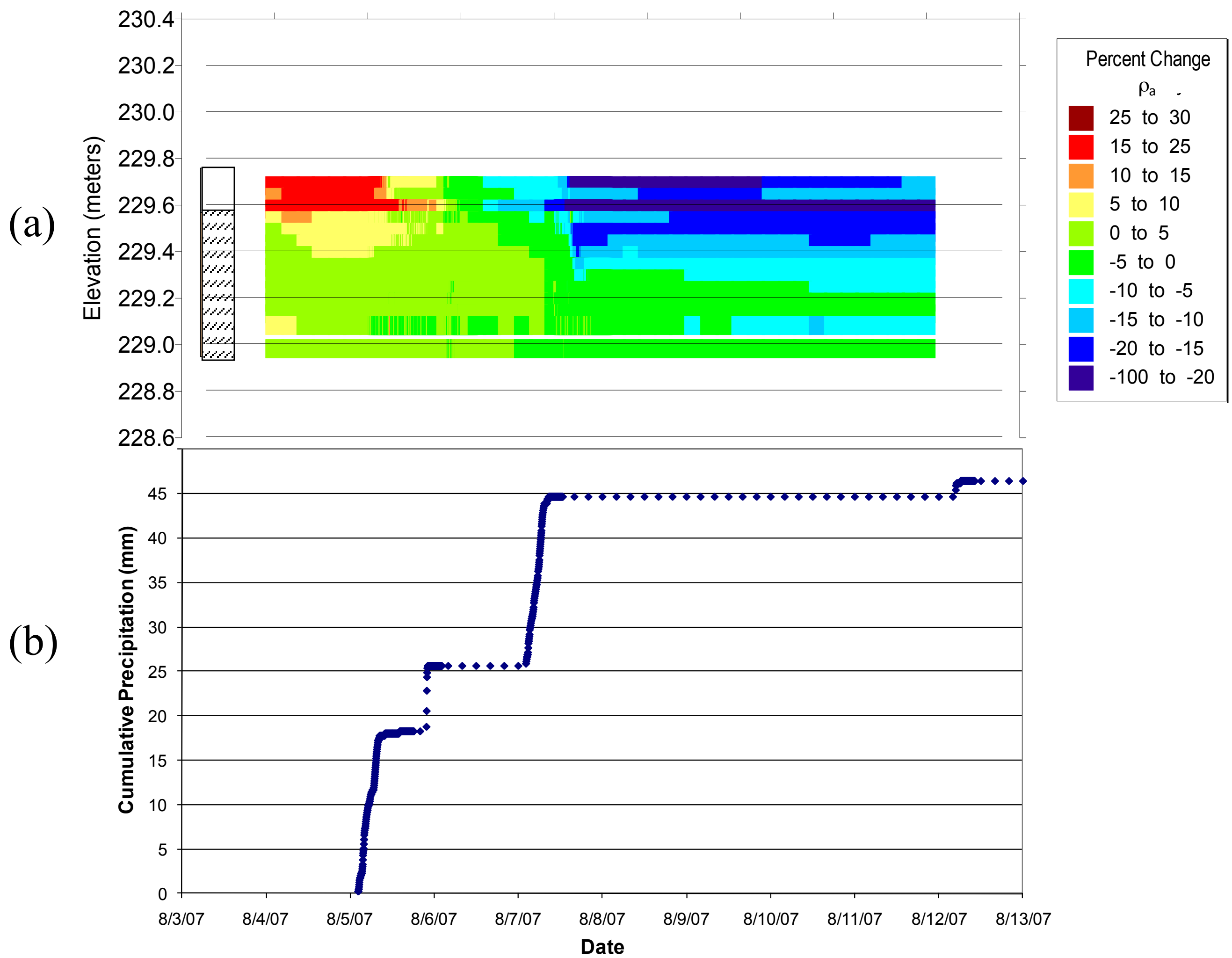

Figure 6: High resolution (time scale of one week) infiltration front imaging at Probe 1 as imaged through (a) % change ρ_a and (b) the cumulative precipitation for the 5-13 Aug 2007 precipitation event.

Temperature Dependence

There is an obvious correlation between the weekly average temperature and the measured apparent resistivity in Figure 4, which is expected since temperature influences apparent resistivity. Apparent resistivity decreases during the summer months due to increased temperatures and increases during the winter months due to decreased temperatures. Keller and Frischknecht (1966) indicate theoretical temperature dependency of electrolyte or rock saturated with electrolyte in the following formula:

$$\rho_t = \frac{\rho_{18}}{1 + \alpha_t(t - 18°)}$$

where ρ_{18} is the reference resistivity at 18°C (although other temperatures may be used), α_t is the temperature coefficient of resistivity (typically 0.025/°C), t is the changed temperature, and ρ_t is the resistivity at the changed temperature. This work was advanced in low-temperature geologic environments, within the range of 0-25°C, by Hayley et al. (2007). These researchers performed laboratory experiments and a field study showing a 1.8% to 2.2% change in the bulk electrical conductivity per degree Celsius, which should be considered a representative approximation, in the absence of other information (Hayley et al., 2007). Using a reference resistivity of 160Ωm at 18°C and solving for the resistivity at 8°C using the formula presented by Keller and Frischknecht, a percent change in the electrical conductivity of 2.5% per degree Celsius is obtained. The above reference resistivity and temperature values were chosen because they fall within the range of data collected at our field site.

We tested these approximations by selecting reference values from our vadose zone and saturated zone data and determined empirical temperature coefficients for these two zones. A sample of data was taken between 5 March 2007 and 28 May 2007, which consisted of a total of 500 data points from the normal data collection mode, to derive an empirical relationship between the temperature and the bulk electrical conductivity at the location of Probe 1. Our empirically derived relationship using subsurface temperatures measured by the probe thermistors shows a 2.98% change of conductivity per degree Celsius in the saturated zone and a 5.27% change of conductivity per degree Celsius in the vadose zone. Recall, these percent changes were calculated with respect to the apparent resistivity measured on 13 May 2007. This date was chosen because a measurement of the pore water conductivity was made on this date. The saturated zone response was determined from data at the lowest five measurement positions. The unsaturated zone response was determined from the data collected at the upper six measurement positions. This temperature correction was applied to the apparent resistivity values of Probe 1 between December 2006 and August 2007.

Apparent resistivity values from 228.98 m elevation at the location of Probe 1 from 24 December 2006 through 31 August 2007 were corrected for temperature and are displayed in Figure 7. The measurement position shown in this figure remained below the water table for the duration of the time range plotted. As such it may be assumed that the apparent resistivity was not impacted by saturation changes. The most likely changes at this position would be caused by changes in temperature or pore water conductivity variations. At this elevation of Probe 1, the overall range of temperature-corrected apparent resistivity observed between 24 December 2006 and 31 August 2007 is 61.42 Ωm to 68.49 Ωm. As the overall apparent resistivity at this position remains fairly constant, we assume that the pore water conductivity does not significantly vary over the sampled time interval. Figure 8 shows similar results at an elevation of 229.63 m at Probe 1 and depicts measurements made in the vadose zone. The temperature-corrected apparent resistivity is influenced by the variation of vadose zone water content. Thus interpretations concerning the saturation state of the subsurface may be made from Figure 8.

Interestingly, a marked increase of apparent resistivity is noted in June and July when the apparent resistivity is corrected for temperature variations (Figure 8), despite the fact that the apparent resistivity is expected to decrease during the summer months from increased surface temperatures. This phenomenon is likely caused by the depletion of soil moisture in the root zone due to extraction by vegetation which is exactly what Michot et al. (2003) and Panissod et al. (2001) observed during summer months. Therefore, an accurate quantitative analysis of the moisture content of the subsurface would require the use of temperature corrections.

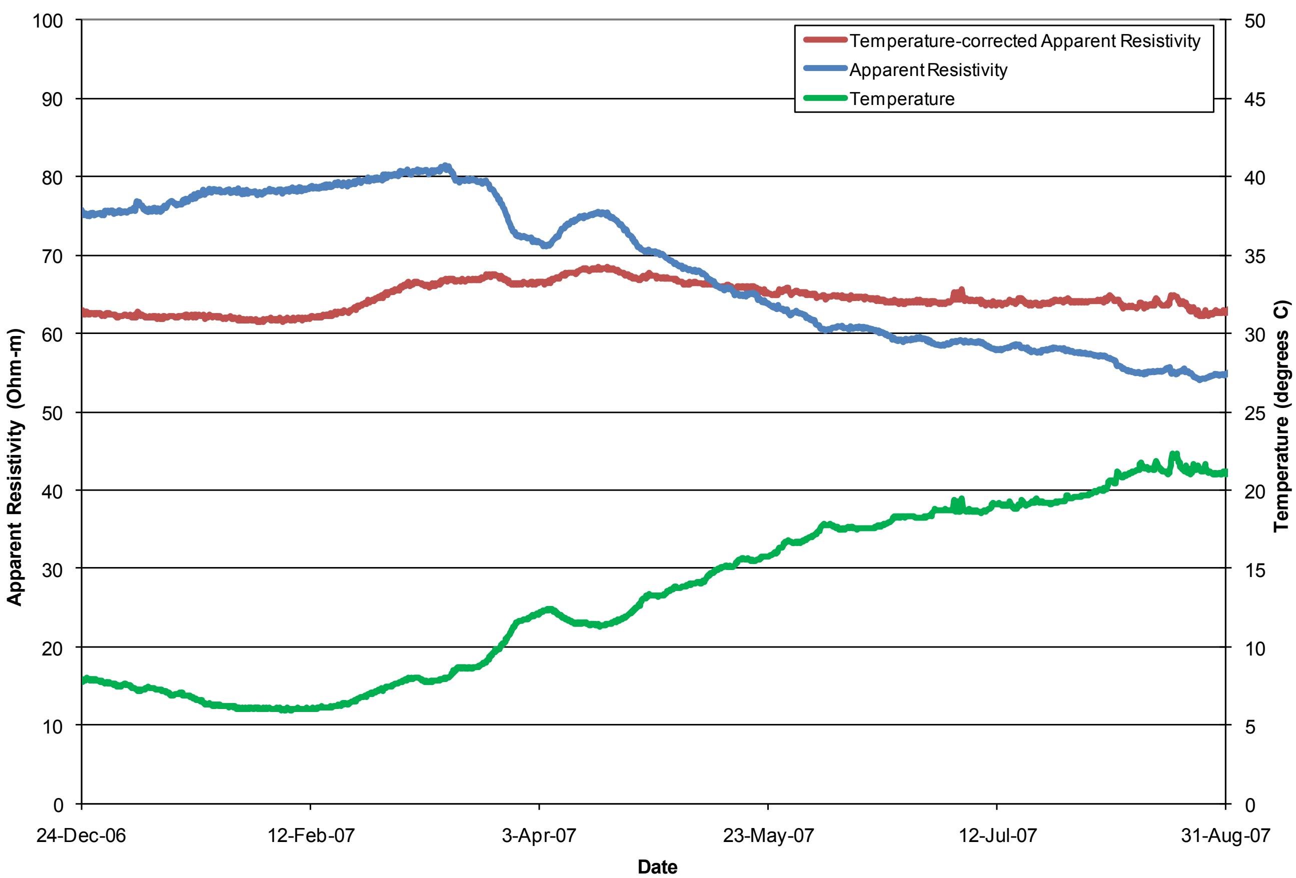

Figure 7: Saturated zone temperature-corrected apparent resistivity.

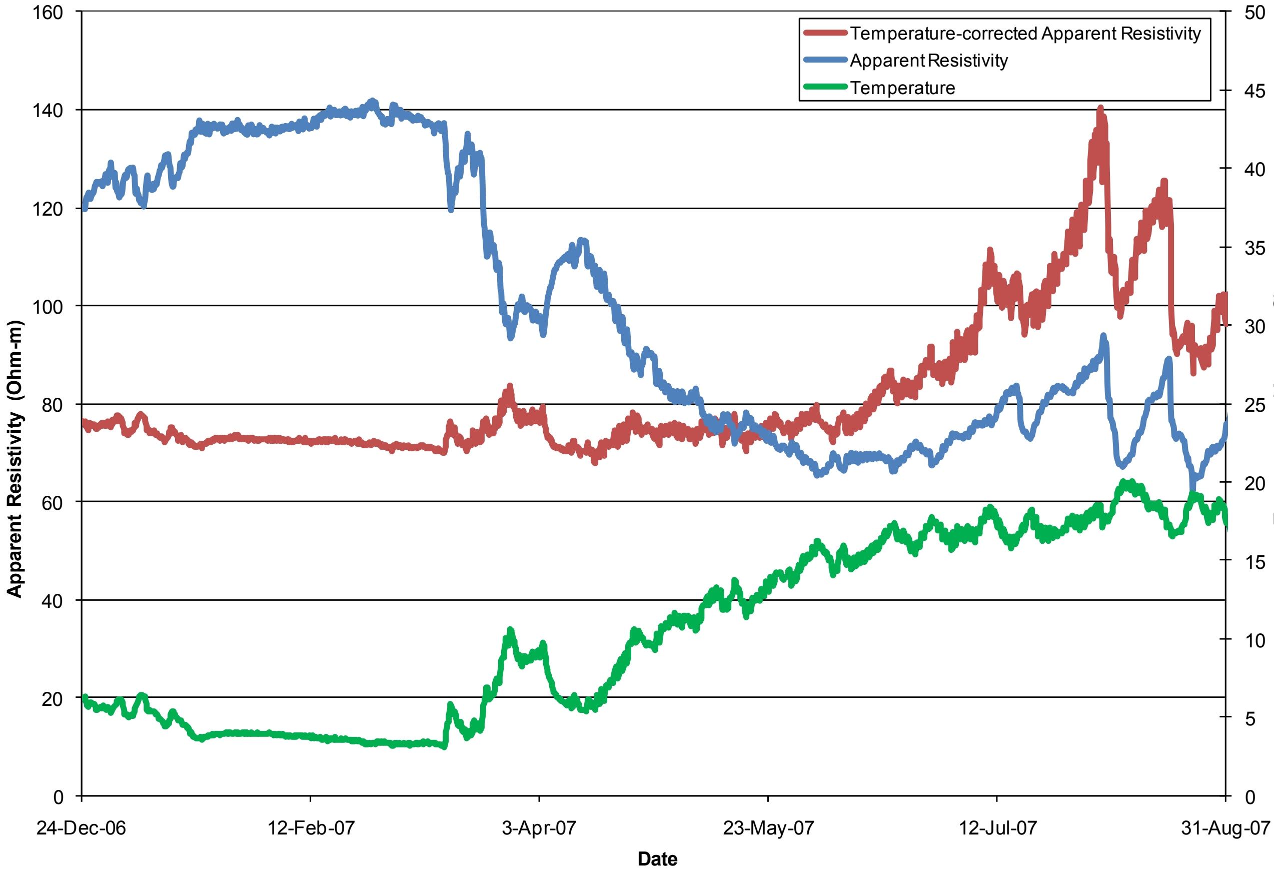

Figure 8: Vadose zone temperature-corrected apparent resistivity.

Volumetric Water Content Limitations

It is very useful to convert apparent resistivity measurements to volumetric water content. However, this conversion requires a valid field measurement of volumetric water content in order to correlate to the field measurements of apparent resistivity or an inversion of the data is necessary to apply Archie's Law for a reasonable estimate. Due to the presence of pebbles and cobbles in the subsurface at this site, the use of time domain reflectometry (TDR) or a neutron probe for measuring the subsurface water content is impractical. These instruments require a calibration to the volumetric water content of an undisturbed soil sample. Samples taken of the soil at this site contain large pebbles that radically alter the calculated volumetric water content. For this specific site, apparent resistivity proved a practical method of monitoring the subsurface water content variation over a testing period of nearly three years. A general understanding of the water content may be obtained in heterogeneous subsurfaces such as the one encountered at this site through the use of the resistivity index, which is defined as the observed resistivity divided by the saturated resistivity. However, this requires foreknowledge of the resistivity at saturation for each measurement position. Alternatively, as shown in this work, the percent change of apparent resistivity can be used to qualitatively image the saturation state of the subsurface in the absence of a true calibration between volumetric water content and resistivity.

4.0 Conclusions

The method presented in this work details an example of a low-cost system of making long-term subsurface apparent resistivity and temperature measurements in a shallow field setting. The system contains low-cost commercially available components and proved durable over the course of nearly three years. High quality, high resolution data were collected at a moderately heterogeneous, shallow subsurface location. The electrode spacing of 5 cm allowed an intricate depiction of the infiltration of precipitation in a natural field setting, while the durable nature of the system allowed long-term observations. The short-term, high temporal resolution, data collection during and after precipitation events clearly shows imbibition and drainage due to natural infiltration events. Seasonal trends are observed in the long-term apparent resistivity data as temperature variations, with high apparent resistivity values in the winter months and low apparent resistivity values in the summer months, and infiltration patterns, which are influenced by the seasonal variation in precipitation form (rain versus snow) and ground cover (grass versus snow). Subsurface temperature variability impacted field resistivity measurements, especially over long time periods. At the field site analyzed in this study, the variation of conductivity with temperature was a 2.97% increase of conductivity per degree Celsius in the saturated zone and a 5.27% increase of conductivity per degree Celsius in the vadose zone.

Apparent resistivity has been shown to monitor infiltration fronts and to identify water uptake by plant roots. As an extension to the applicability of this system, resistivity could, in some circumstances, be used to determine useful hydrogeological parameters such as water content in the vadose zone, but only if resistivity can be previously calibrated against absolute water content at the same site. Likewise, the low-cost system described herein could be applied to low-budget projects which may require the monitoring of either subsurface water content or chemical changes of subsurface water which may be correlated to resistivity changes and possible agricultural studies of plant water uptake.

5.0 Acknowledgements

Funding for this project was provided by the Michigan Space Grant Consortium Graduate Research Fellowship. The authors wish to thank Mr. Rockie Keeley for the use of his land as a field test site. Although this work was reviewed by EPA and approved for presentation, it may not necessarily reflect official Agency policy. Mention of trade names or commercial products does not constitute endorsement or recommendation by EPA for use. We also appreciate the comments from reviewers, which strengthened and clarified this manuscript.

References

Aaltonen, J. and B. Olofsson. 2002. Direct current (DC) resistivity measurements in long-term groundwater monitoring programmes. *Environmental Geology*, 41(6): 662-671.

Atekwana, E.A., W.A. Sauck, and D.D. Werkema, Jr. 2000. Investigations of geoelectrical signatures at a hydrocarbon contaminated site. *Journal of Applied Geophysics*, 44: 167-180.

Binley, A., G. Cassiani, R. Middleton, and P. Winship. 2002a. Vadose zone flow model parameterisation using cross-borehole radar and resistivity imaging. *Journal of Hydrology*, 267: 147-159.

Binley, A., P. Winship, L.J. West, M. Pokar, and R. Middleton. 2002b. Seasonal variation of moisture content in unsaturated sandstone inferred from borehole radar and resistivity profiles. *Journal of Hydrology*, 267: 160-172.

Cassiani, G., V. Bruno, A. Villa, N. Fusi, and A.M. Binley. 2006. A saline trace test monitored via time-lapse surface electrical resistivity tomography. *Journal of Applied Geophysics*, 59: 244-259.

Daily, W. and A. Ramirez. 1995. Electrical resistance tomography during in-situ trichloroethylene remediation at the Savannah River Site. *Journal of Applied Geophysics*, 33: 239-249.

Grimm, R.E., G.R. Olhoeft, K. McKinley, J. Rossabi, and B. Riha. 2005. Nonlinear Complex-Resistivity Survey for DNAPL at the Savannah River Site A-014 Outfall. *Journal of Environmental and Engineering Geophysics*, 10(4): 351-364.

Groncki, J.M. and W.A. Sauck. 2000. Calibration, installation techniques, and equilibration considerations for vertical resistivity probes used in hydrogeologic investigations, Symposium on the Application of Geophysics to Engineering and Environmental Problems, pp. 979-988.

Hagrey, S.A. and J. Michaelsen. 1999. Resistivity and percolation study of preferential flow in vadose zone at Bokhorst, Germany. *Geophysics*, 64(3): 746-753.

Hayley, K., L. Bentley, M. Gharibi, and M. Nightingale. 2007. Low temperature dependence of electrical resistivity: Implications for near surface geophysical monitoring. *Geophysical Research Letters*, 34: L18402.

Johnson, T., R. Versteeg, H. Huang, and P. Routh. 2009. Data-domain correlation approach for joint hydrogeologic inversion of time-lapse hydrogeologic and geophysical data. *Geophysics*. 74: F127-F140.

Keller and Frischknecht. 1966. *Electrical Methods in Geophysical Prospecting*. Oxford: Pergamon Press.

Kemna, A., J. Vanderborght, B. Kulessa, and H. Vereecken. 2002. Imaging and characterisation of subsurface solute transport using electrical resistivity tomography (ERT) and equivalent transport models. *Journal of Hydrology*, 267: 125-146.

LaBrecque, D. and W. Daily. 2008. Assessment of measurement errors for galvanic-resistivity electrodes of different composition. *Geophysics*, 73(2): F55-F64.

LaBrecque, D. and R. Sharpe. 2006. Progress in Ultra-High Precision Resistivity Tomography: Electrode Aging in Long-Term Monitoring. Symposium on the Application of Geophysics to Engineering and Environmental Problems, pp. 639-646.

Linde, N., A. Binley, A. Tryggvason, L.B. Pedersen, and A. Revil. 2006. Improved hydrogeophysical characterization using joint inversion of cross-hole electrical resistance and ground-penetrating radar traveltime data. *Water Resources Research*, 42: W12404.

Michot, D., Y. Benderitter, A. Dorigny, B. Nicoullaud, D. King, and A. Tabbagh. 2003. Spatial and temporal monitoring of soil water content with an irrigated corn crop cover using surface electrical resistivity tomography. *Water Resources Research*, 39(5): 14-1 - 14-20.

Narbutovskih, S.M., W. Daily, A.L. Ramirez, T.D. Halter, and M.D. Sweeney. 1996. Electrical resistivity tomography at the DOE Hanford site, Symposium on the Application of Geophysics to Engineering and Environmental Problems, pp. 773-782.

Nichols, G. 1999. Sedimentology & Stratigraphy: Cambridge, University Press, 355 p.

Ogilvy, R., P. Meldrum, O. Kura, P. Wilkinson, J. Chambers, M. Sen, A. Pulido-Bosch, J. Gisbert, S. Jorreto, I. Frances, and P. Tsourlos. 2009. Automated monitoring of coastal aquifers with electrical resistivity tomography. *Near Surface Geophysics*, 7: 367-375.

Panissod, C., D. Michot, Y. Benderitter, and A. Tabbagh. 2001. On the effectiveness of 2D electrical inversion results: an agricultural case study. *Geophysical Prospecting*, 49: 570-576.

Pfiefer, M.C. and H.T. Andersen. 1995. DC-resistivity array to monitor fluid flow at the INEL infiltration test, Symposium on the Application of Geophysics to Engineering and Environmental Problems, pp. 709-718.

Reed, P.C., P.B. DuMontelle, M.L. Sargent, and M.M. Killey. 1983. Nuclear Logging and Electrical Earth Resistivity Techniques in the Vadose Zone in Glaciated Earth Materials, NWWA/U.S. EPA conference on characterization and monitoring of the vadose (unsaturated) zone, pp. 580-601.

Sauck, W.A. 2000. A model for the resistivity structure of LNAPL plumes and their environs in sandy sediments. *Journal of Applied Geophysics*, 44: 151-165.

Singha, K. and S. Gorelick. 2005. Saline tracer visualized with three-dimensional electrical resistivity tomography: Field-scale spatial moment analysis. *Water Resources Research*, 41: W05023.

Singha, K. and S. Gorelick. 2006a. Effects of spatially variable resolution on field-scale estimates of tracer concentration from electrical inversions using Archie's law. *Geophysics*, 71(3): G83-G91.

Singha, K. and S. Gorelick. 2006b. Hydrogeophysical tracking of three-dimensional tracer migration: The concept and application of apparent petrophysical relations. *Water Resources Research*, 42: W06422.

Stephens, D.B. 1996. *Vadose Zone Hydrology*. Boca Raton, FL: CRC Press, Inc.

Vanderborght, J., A. Kemna, H. Hardelauf, and H. Vereecken. 2005. Potential of electrical resistivity tomography to infer aquifer transport characteristics from tracer studies: A synthetic case study. *Water Resources Research*, 41: W06013.

Werkema, D. 2002. Geoelectrical Response of an Aged LNAPL Plume: Implications for Monitoring Natural Attenuation. Ph.D. diss., Department of Geology, Western Michigan University.

Werkema, D.D., E.A. Atekwana, E.A. Atekwana, J. Duris, J. Allen, L. Smart, and W.A. Sauck. 2004. Laboratory and field results linking high bulk conductivities to the microbial degradation of petroleum hydrocarbons, Symposium on the Application of Geophysics to Engineering and Environmental Problems, pp. 363-373.

Yang, X. and D. LaBrecque. 2000. Estimation of 3-D moisture content using ERT data at the Socorro-Tech Vadose Zone Facility, Symposium on the Application of Geophysics to Engineering and Environmental Problems, pp. 915-924.